China Instrument and Control Society
Instrumentation

OPEN ACCESS

INSTRUMENTATION, Vol. 13, No. 2, June 2026 https://doi.org/10.15878/j.instr.202600332

Article

Generalized Ellipsometry Measurement based on Variable Angle Driven by Single Motor

Peng Xue[1,2*], Quanlong Yang[1,2], Rui Zhang[2], Zhibin Wang[2]

[1] School of Electrical and Control Engineering, North University of China, Taiyuan 030051, Shanxi Province, China

[2] Technology Innovation Center of Shanxi Provincial for Intelligent Microwave Photoelectric, Taiyuan 030051, Shanxi Province, China

[*] Corresponding author email: xuepeng@nuc.edu.cn

Abstract: With the advancement of microelectronics, semiconductors, and nanotechnology, thin-film materials have found extensive applications in electronic and optical components. The thin-film thickness serves as a critical parameter affecting the performance and reliability of such components. For rapid, non-destructive, and precise thickness measurements, generalized ellipsometers have attracted considerable research. However, commercially available ellipsometers typically require two motors to realize the variable angle (one to control the polarization state generator/analyzer, and another to rotate the sample stage). This conventional design suffers from complex structure, high cost and difficulty in optical path calibration after angle variation. To address these limitations, a novel variable angle structure driven by single motor is proposed in this paper, in which the polarization state generator is fixed and the polarization state analyzer and the sample stage are driven simultaneously using single motor to realize the variable angle. Using the developed system, standard thin-film samples of Au, Ag, and Cu, each with a nominal thickness of 50 nm, were tested. The results indicated that the thicknesses of the three samples fell within the range of 50±2 nm. Furthermore, the system exhibited minimal measurement error at an incident angle of 70°. These findings demonstrate that the proposed ellipsometry system with variable angle driven by single motor offers higher integration, simpler operation, and lower cost compared to traditional dual-motor designs.

Keywords: generalized ellipsometry; thin-film measurement; single-motor drive

Copyright: © 2026 by the authors. This article is licensed under a Creative Commons Attribution 4.0 International License (CC BY) license (https://creativecommons.org/licenses/by/4.0/).

Citation: Peng Xue, Quanlong Yang, Rui Zhang, Zhibin Wang."Generalized Ellipsometry Measurement based on Variable Angle Driven by Single Motor." Instrumentation 13, no.2 (June 2026). https://doi.org/10.15878/j.instr.202600332

1 Introduction

Along with the development of the nanotechnology, integrated circuits, flat-panel displays and semiconductor technology, nano-materials have been widely used in various fields [1-3]. As a common nano-material, metal-film plays an important role in the application of nanotechnology. For example, metal-films are used in optical fiber communication to prepare inductive filters, short-wave communication films, and depolarizing beam splitters with superior performance. In micro-electro-mechanical systems (MEMS) manufacturing, metal-films are used as electrodes and seed layers [4]. Measuring the thickness of a metal-film quickly, accurately, and non-destructively is significant to improving the industry's production efficiency and product performance.

The measurement methods of metal-film thickness are roughly divided into non-optical and optical methods. Non-optical methods mainly include high-precision microscopic measurements, probe measurements, etc. [5]. Among them, high-precision microscopic measurement mainly uses transmission electron microscope (TEM), scanning electron microscope (SEM), atomic force microscope (AFM), etc.[6,7], which have the advantages of

high measurement accuracy but have complicated operation, high cost, slow measurement speed, and contact measurement that may damage the sample. The probe measurement method employs an easy-to-operate probe profiler with a much more extensive scanning range than microscopes for measurements. Owing to the need for secondary processing of the sample, however, it is easy to damage the sample's surface, and non-destructive testing cannot be achieved [8]. Optical methods mainly include ray thickness, laser thickness, optical interference thickness, ellipsometry thickness measurements, etc. Among them, the ellipsometry method analyzes and extracts parameters (such as film thickness, optical constants) of the sample by measuring the change of polarization characteristics of polarized light before and after being incident on the sample. It has become the most widely used method because of its high precision, high sensitivity, and non-contact [9-11].

At present, the common types of ellipsometers include a rotary analyzer, rotary polarizer, and single-rotation compensator. These ellipsometers have simple structures, a wide range of incident angles, and a broad measurement spectrum. In a single measurement, however, only partial elements of the Mueller matrix of the sample can be obtained. Additionally, the method is only suitable for measuring isotropic samples[12-14]. In 1978, Professor Azzam[15] proposed a dual rotating compensator ellipsometry measurement technology. By setting a specific rotational speed ratio to the two retarders, all 16 elements of the Mueller matrix were obtained for the first time. In 1999, R. W. Collins et al.[16] proposed a dual-rotating compensator multi-channel generalized ellipsometer and made a detailed theoretical analysis of its use for fast measurement of surface thin films. In 2008, G. Piller et al [17] studied the systematic errors due to azimuth shifts of the polarizer, analyzer and two compensators in a dual rotating-compensator Mueller matrix ellipsometry. In 2016, W. Q. Li et al [18] studied the depolarization artifacts in dual rotating compensator Mueller matrix ellipsometry. In 2023, J. Qi et al [19] proposed an error correction method based on a reference optical path for Mueller matrix ellipsometry. So far, these are commercially available generalized ellipsometer based on dual rotating compensator on the market, such as VASE type wide-spectrum generalized ellipsometer developed by the J. A. Woollam Co, ME-L type generalized ellipsometer developed by the Wuhan eoptics Technology Co., Ltd, EGS02 type generalized ellipsometer developed by the ELLITOP Scientific Co., Ltd, and so on.

However, the implementation of the angle changing function for the current commercial generalized ellipsometers are usually driven by two motors, one is used to control the polarization state generator/analyzer, and the other is used to control the sample stage, which will lead to a high cost and need for precise coordinated control of the dual-motor to ensure measurement accuracy. Compared with the dual-motor control, the proposed variable angle structure driven by single motor offers cost-effectiveness, integration simplicity, ease of calibration—without compromising measurement capability. To further verify the performance of the built generalized ellipsometry system, different metal-films were tested.

2 Measurement Principle

The schematic of the generalized ellipsometry measurement based on the dual rotating-compensators is shown in Fig. 1, where C_1 and C_2 represent the first and second rotary compensators, respectively.

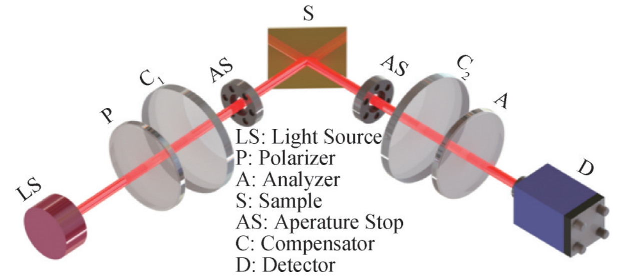

Fig.1 Schematic diagram of generalized ellipsometry measurement based on dual rotating compensators

When the beam passes through the elements P, C_1, and S, C_2, and A, the Stokes vector of the outgoing beam can be expressed as $\boldsymbol{S_{out}}$ [20]:

$$S_{out}=\left[M_A R(A)\right]\left[R(-C_2)M_{C2}(\delta_2)R(C_2)\right]\times M_S\times \left[R(-C_1)M_{C1}(\delta_1)R(C_1)\right]\left[R(-P)M_P\right]S_{in} \quad (1)$$

where $\boldsymbol{S_{in}}$ is the Stokes vector of the beam before entering the polarizer, M_P and M_A are the Mueller matrices of the polarizer and analyzer, respectively. $M_{C1}(\delta_1)$ and $M_{C2}(\delta_2)$ are the Mueller matrices of the compensators C_1 and C_2, when the phase retardations are δ_1 and δ_2, respectively. M_S is the Mueller matrix of the sample, and $R(\alpha)$ is the rotated Mueller matrix when the azimuth angle of the element relative to the incident surface is α. The first element of $\boldsymbol{S_{out}}$ is the light intensity $\boldsymbol{I}$ detected by the detector, which can be expressed as:

$$I=I_0\{K_1+\left[c_2\cos 2A+s_2\cos(4C_2-2A)\right]K_2 +\left[c_2\sin 2A+s_2\sin(4C_2-2A)\right]K_3 -\sin\delta_2\sin 2(C_2-A)K_4\} \quad (2)$$

where,

$$K_j=m_{j1}+\left[c_1\cos 2P+s_1\cos(4C_1-2P)\right]m_{j2} +\left[c_1\sin 2P+s_1\sin(4C_1-2P)\right]m_{j3} +\sin\delta_1\sin 2(C_1-P)m_{j4} \quad (3)$$

and $c_j=\cos^2(\delta_j/2)$, $s_j=\sin^2(\delta_j/2)$, $m_{jk}(j=1,\cdots,4;\ k=1,\cdots,4)$. By performing Fourier analysis on $\boldsymbol{I}$, and parallel calculations with Eq. (2), all 16 elements m_{jk} of the Mueller matrix of the sample can be deduced.

The Mueller matrix of the isotropic metal-film

samples can be expressed as:

$$M_S = \begin{bmatrix} 1 & -N & 0 & 0 \\ -N & 1 & 0 & 0 \\ 0 & 0 & C & L \\ 0 & 0 & -L & C \end{bmatrix} \tag{4}$$

where the relationship between N, L, C and the ellipsometry parameters (Ψ, Δ) is as follows: N=cos(2Ψ), L=sin(2Ψ)sinΔ, C=sin(2Ψ)cosΔ. Since sine and cosine functions describe N, L, and C, they are between −1 and 1. The Experimental measurements of ellipsometry parameters Ψ and Δ in m_{jk} are obtained through the relationship between N, L, C, and the ellipsometry parameters.

Selecting a suitable model is the key to preparing the ellipsometry film thickness measurement. This paper uses the Lorentz dispersion model to model the Au, Ag, and Cu films. The dielectric constant ε can be expressed as [21]:

$$\varepsilon(\omega)=\varepsilon_\infty+\frac{\omega_p^2}{(\omega_0^2-\omega^2)-i\omega\gamma} \tag{5}$$

where ω_0 is the natural oscillation frequency of the metal. ε_∞, γ, ω_p, and ω_0 are related to the frequency of incident light and determined by fitting. According to Eq. (5), the fitting results of the dielectric constants ε of Au, Ag, and Cu are shown in Fig. 2. It can be seen that the fitting results of Au, Ag, and Cu are consistent with their theoretical ε values. By determining ε, the optical constants of the metal-film that continuously change with wavelength can be obtained, including the refractive index n and extinction coefficient k[22], and then the theoretical Ψ and Δ values can be calculated.

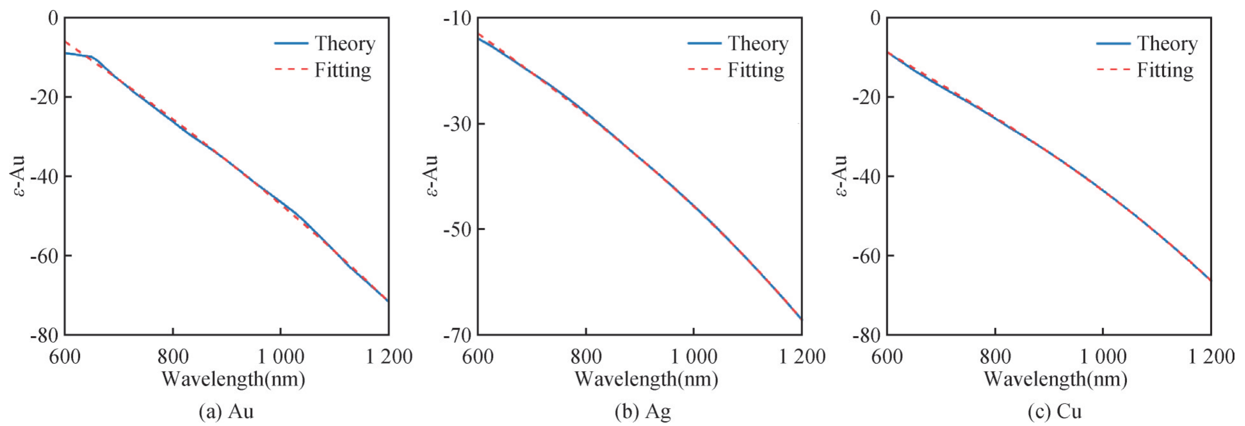

Fig.2 Fitting results of ε for metal-films: (a) Au, (b) Ag, and (c) Cu

When the incident wavelength λ and incident angle θ are determined, the ellipsometry parameters Ψ and Δ are functions of the refractive index n, extinction coefficient k, and film thickness d of the thin-film sample, that is, $\Psi = f(n, k, d)$ and $\Delta = g(n, k, d)$. Through regression analysis, the theoretically generated Ψ and Δ are compared with the experimentally measured Ψ and Δ, and the measured values of Ψ and Δ are fitted by constantly changing n, k, and d. When the fitted Ψ and Δ are in good agreement with the measured Ψ and Δ, the d of the metal-film sample is finally obtained.

3 Variable Angle Principle and Structure Driven by Single Motor

The multi-angle measurement of the ellipsometer proposed in this paper is achieved by fixing the polarization state generator (PSG), rotating the polarization state analyzer (PSA) and the sample stage synchronously by single motor. To ensure the collimation of the optical path after each angle change, the rotation angle β of PSA and the rotation angle α of the sample stage should be satisfied as β=2α, as shown in Fig. 3, where N is the normal of the sample surface when the PSA is in its initial state (β=0°). γ is the incidence angle when the rotation angle of the PSA is β , and the normal is N'.

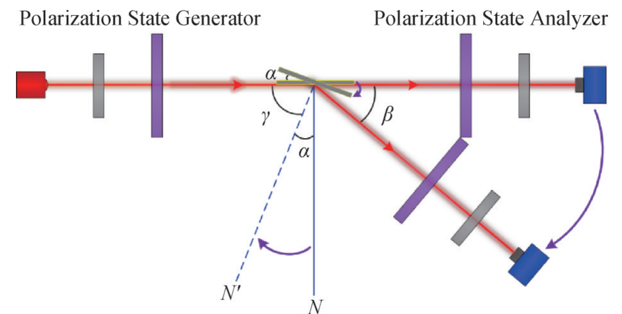

Fig.3 Schematic diagram of the variable angle principle

The schematic of the variable angle structure driven by single motor is shown in Fig. 4. The main axis of the motor is connected with the PSA and the gear 1 to drive the PSA to rotate. The gear 2 with the same number of teeth as gear 1 is driven by gear 1. The gear 3, which is coaxial with gear 2, drives gear 4 to rotate to realize the rotation of the sample stage. In order to keep the collimation of the optical path during the angle change, according to the Fig. 3, the ratio of the number of teeth between gear 3 and 4 is set to 2:1. Thus, the sample stage and the PSA rotate synchronously at a speed ratio of 1:2

to maintain real-time optical alignment. The structure shown in Fig. 4 not only ensures a compact overall structure of the system, but also reduces alignment time in comparison with the traditional horizontal variable angle structure that requires high-precision coordinated control of dual-motor to maintain optical alignment.

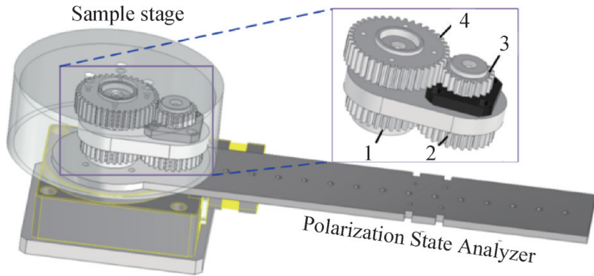

Fig.4 Schematic of the variable angle structure driven by single motor

4 Experiment

The generalized ellipsometry system constructed according to the principle shown in Fig. 1 and Fig. 3 is shown in Fig. 5. The light source (MDL-XS-635 nm, Changchun New Industry Optoelectronics Technology Co., Ltd., Changchun, China) uses a laser with a wavelength of 635 nm . The polarizer P and analyzer A use a Rochon prism (RPM10, THORLABS, Newton, NJ, USA), the compensators C_1 and C_2 are achromatic λ/4-wave plates (WPA-4-15-400-100-DZ, Beijing Liangtuo Technology Co., Ltd.), and a photodetector (Model PDA10A-EC, THORLABS Inc., Newton, New Jersey, USA) detects the output light intensity. The thin-film samples are selected as standard samples of silicon-based Au, Ag, and Cu, and the coating thickness is 50± 3 nm.

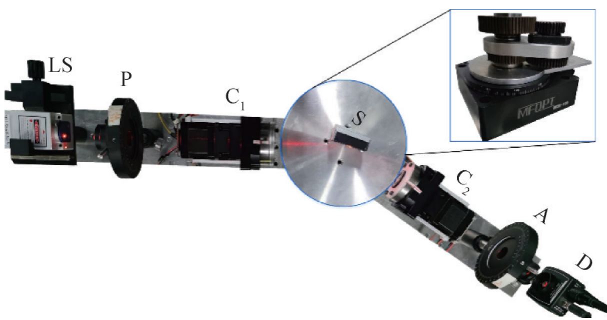

Fig.5 The generalized ellipsometry system with variable angle driven by single motor

According to the device shown in Fig. 5, two compensators are mounted inside hollow stepping motors (Model 42, Fujian Xinxuan Electronic Technology Co., Ltd., Fujian, China) and rotate synchronously at an angular frequency ratio of ω_1: ω_2=5: 3, and the standard samples of Au, Ag, and Cu are tested. In the two optical cycles, the change of the collected light intensity as the modulation time is shown in Fig. 6, indicating that the collected light intensity is relatively stable.

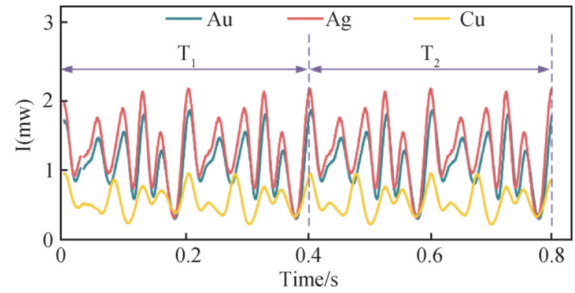

Fig.6 Light intensity versus modulation time

Substituting the light intensity in Fig. 6 into Eq. (2), the obtained Mueller matrices of the Au, Ag, and Cu samples at different incident angles are shown in Fig. 7. It can be seen that the distribution of Mueller matrix element values of Au, Ag, and Cu films is relatively regular, and when the incident angles are 60°, 65°, and 70° , the Mueller matrix element values are closer. However, when the incident angle is 75°, the elements of the Mueller matrix change significantly. This is because the ellipsometry parameters Ψ and Δ change significantly when the incident angle is near the Brewster angle, and the measurement is also more sensitive [23].

According to Eq. (4), the ellipsometry parameters obtained by the experimental measurement are shown in Fig. 8. To measure the thickness of the metal-film, the simulated annealing algorithm. [24] programmed in MATLAB R2025b (MathWorks, Natick, MA, USA) is used to perform numerical iterative fitting on the experimental ellipsometry parameters Ψ and Δ, and the fitting results are shown in Fig. 8. It can be seen that the fitting results are basically consistent with the experimental model. It can also be seen from Fig. 8 that both Ψ and Δ show a decreasing trend with the increase of the incident angle θ, where Ψ changes slightly with θ, while Δ changes significantly. This shows that the variation of Δ with θ is obviously sensitive to Ψ. That is, in ellipsometry data processing, when calculating the film thickness d, the accuracy of the ellipsometry parameter Δ is more important than the accuracy of Ψ. Since the ellipsometry parameters change greatly near the Brewster angle, it can also be seen from the figure that the Brewster angle of the metal-film sample is around 70°.

The thickness fitting result of the metal-film is shown in Fig. 9. It can be seen that when the incident angle is 70°, the measured value is closer to the true value of the sample thickness, indicating that the fitting effect is the best near 70° and confirms the speculation that Brewster's angle is around 70°.

Table 1 lists the absolute error of thickness d. The thickness fitting error of Au and Cu samples is less than 1nm, while the thickness fitting error of the Ag sample is less than 2nm. Au and Cu samples had relatively better thickness fitting results than Ag samples. The potential causes include the accuracy of Ag optical constants, surface oxidation effects, or material-dependent sensitivity in the fitting process.

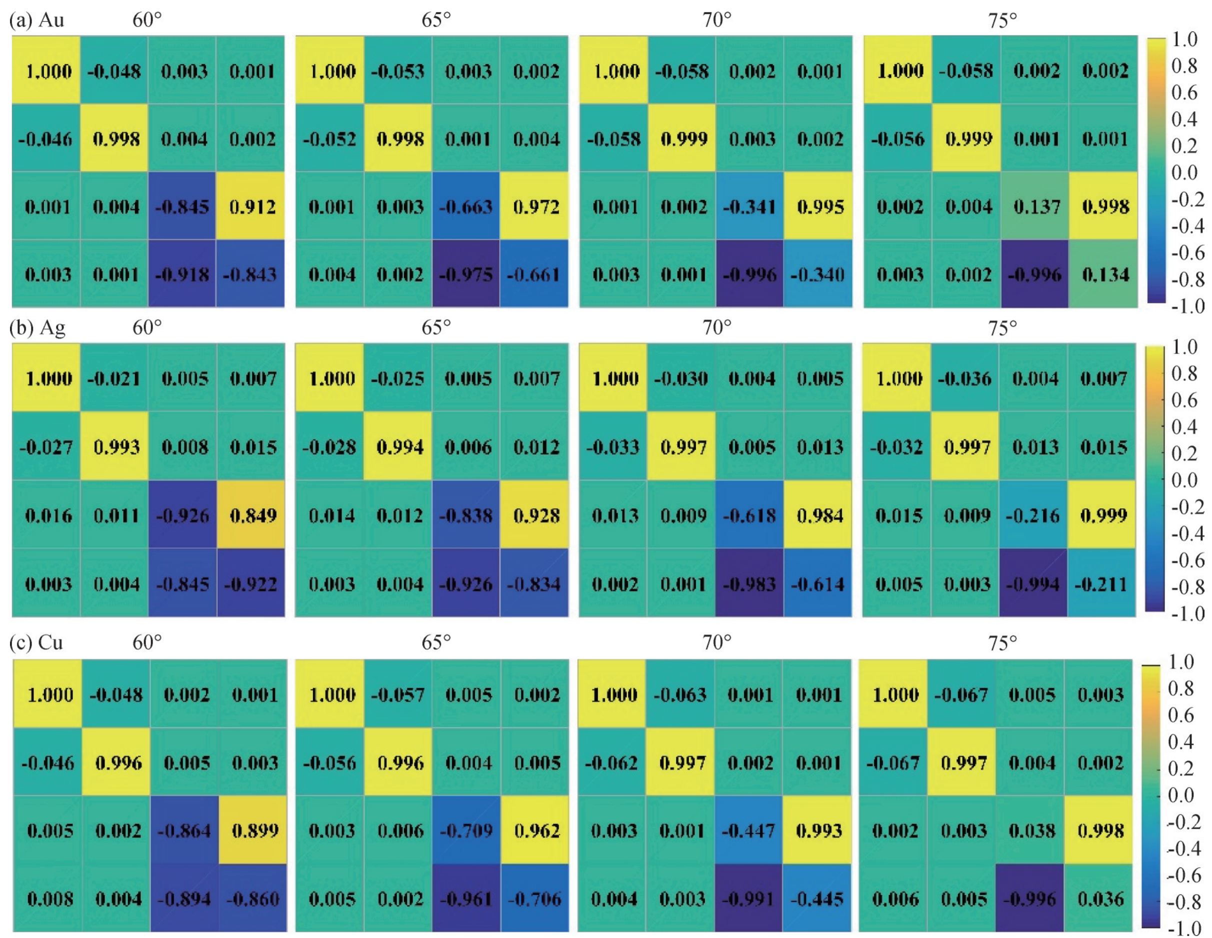

Fig.7 Mueller matrices of metal-film samples at different incident angles: (a) Au, (b) Ag, and (c) Cu

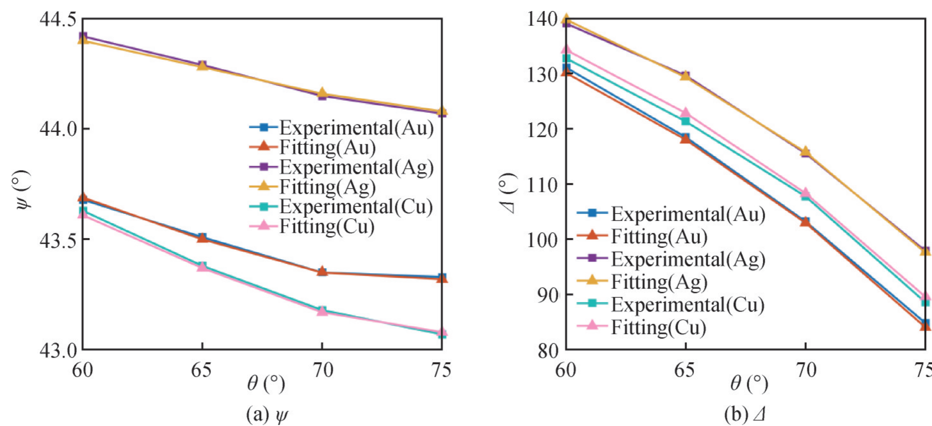

Fig.8 The results of the ellipsometry parameters (a) Ψ and (b) Δ for the metal-film samples at different incident angles

The thickness measurement values of the three metal-film samples are all in the range of 50±2nm, showing the good performance of dual rotating-compensator Mueller matrix ellipsometry in measuring the metal-film thickness. After 30 repeated measurements, the standard deviation for measuring thickness is shown in Table 1. According to the above analysis, to measure the ellipsometry parameters and thickness with higher accuracy, the basic principle for selecting the incident angle choosing the Brewster angle or nearby angles as the incident angle.

5 Conclusion

In this study, a generalized ellipsometry measurement system with the variable angle driven by single motor is proposed, and the self-made ellipsometry system was investigated by testing Au, Ag, and Cu thin-film samples with thicknesses of 50nm at multiple angles. The results show that the variable angle structure driven by single motor has advantages of simple operation, low cost and high precision in optical alignment, and the

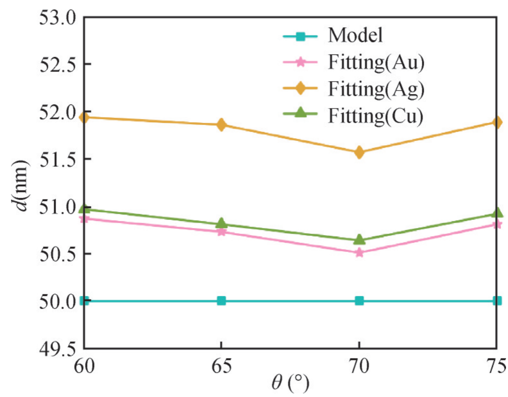

Fig.9 Thickness measurement results of metal-film samples at different incident angles

Table 1 Absolute error and standard deviation of d for metal-film sample

θ	$\lvert d_{Au}\rvert$ (nm)	$\lvert d_{Ag}\rvert$ (nm)	$\lvert d_{Cu}\rvert$ (nm)	σ_{Au}	σ_{Ag}	σ_{Cu}
60°	0.87	1.94	0.97	1.7%	2.5%	1.6%
65°	0.73	1.86	0.81	1.5%	2.1%	1.5%
70°	0.51	1.57	0.64	1.1%	1.9%	1.2%
75°	0.81	1.89	0.92	1.3%	1.9%	1.3%

measurement system can accurately measure the thickness of the metal-film. The thicknesses of the three metal-films are all in the range of 50±2nm, and when the incident angle is 70°, the system measurement error is minimized, showing that measurement system has superior performance in measuring metal-film thickness. It has important academic significance and application value in the engineering process of generalized ellipsometer.

Author Contribution:

Peng Xue: Investigation, Data curation, Methodology, Formal analysis, Visualization. Quanlong Yang: Conceptualization, Software, Writing-original draft. Rui Zhang: Project administration, Funding acquisition, Resources. Zhibin Wang: Data curation, Validation.

Declaration of competing interest:

The authors declare that there is no conflict of interest.

Data Availability:

The authors declare that the main data supporting the findings of this study are available within the paper and its Supplementary Information files.

Foundation Information:

This research was funded by the Central Government Guidance Funds for Local Science and Technology Development Project YDZJSX2025D041.

Dates:

Received 16 October 2025; Accepted 11 May 2026; Published online July 10, 2026.

References

[1] Mehta K P, Sharma R, Haldar S, & Kumar A. (**2023**). Advancement in treatment of wastewater with nano technology [J]. *Materials Today: Proceedings* , 80(P3), 3358-3362. doi: 10.1016/j.matpr.**2021**.07.253.

[2] Ye Z, Su M, Li J, et al. (**2021**). Laser nano-technology of light materials [J]. *Optics and Laser Technology* , 139, 106988. doi: 10.1016/j.optlastec.**2021**.106988.

[3] Saha S, Singh A, Baghini M S, Goel M, & Rao V R. (**2021**). Stand-by Power Reduction Using Experimentally Demonstrated Nano-Electromechanical Switch in CMOS Technologies [J]. *IEEE Transactions on Electron Devices* , 68 (2), 746-752. doi: 10.1109/TED.**2020**.3041434.

[4] Ruffino F. (**2018**). Metallic Films: From Nanofabrication and Nanostructuration to Characterizations and Applications [J]. *Metals* , 8(12), 1018. doi: 10.3390/met8121018.

[5] Zheng D, Yu C, Zhang Q, & Wang H. (**2017**). Evaluating nanoscale ultra-thin metal films by means of lateral photovoltaic effect in metal-semiconductor structure [J]. *Nanotechnology*, 28(50), 505201. doi:10.1088/1361-6528/aa97f5.

[6] Arakawa H, Umemura K, & Ikai A. (**1992**). Protein images obtained by STM, AFM and TEM [J]. *Nature* , 358, 171-173. doi: 10.1038/358171a0.

[7] Fei Z, Rodin A S, Gannett W, et al. (**2013**). Electronic and plasmonic phenomena at graphene grain boundaries [J]. *Nature Nanotechnology* , 8(11), 821-825. doi: 10.1038/nnano.**2013**.197.

[8] Li C, Yang S, Wang Y, Wang C, Ren W, & Jiang Z. (**2016**). Measurement and characterization of a nano-scale multiple-step height sample using a stylus profiler [J]. *Applied Surface Science* , 387, 732-735. doi: 10.1016/j.apsusc.**2016**.06.177.

[9] Jellison G E Jr, & Boat L A. (**1998**). Optical functions of uniaxial ZnO determined by generalized ellipsometry [J]. *Physical Review B* , 58(7), 3586-3589. doi: 10.1103/PhysRevB.58.3586.

[10] Singh M R, Chang Y C, & Wei P K. (**2011**). Ellipsometry study on gold-nanoparticle-coated gold thin film for biosensing application [J]. *Biomedical Optics Express* , 2(9), 2569-2576. doi: 10.1364/BOE.2.002569.

[11] Aspnes D E. (**2014**). Spectroscopic ellipsometry—Past, present, and future [J]. *Thin Solid Films* , 571, 334-344. doi: 10.1016/j.tsf.**2014**.03.056.

[12] Aspnes D E, & Studna A A. (**1975**). High precision scanning ellipsometer [J]. *Applied Optics*, 14(1), 220-228. doi: 10.1364/AO.14.000220.

[13] Kim Y T, Collins R W, & Vedam K. (**1990**). Fast scanning spectroelectrochemical ellipsometry: In-situ characterization of gold oxide [J]. *Surface Science* , 233(3), 341-350. doi:

10.1016/0039-6028(90)90647-Q.

[14] Kleim R, Kuntzler L, & El Ghemmaz A. (**1994**). Systematic errors in rotating-compensator ellipsometry [J]. *Journal of the Optical Society of America A* , 11(9), 2550-2559. doi: 10.1364/JOSAA.11.002550.

[15] Azzam R M. (**1978**). Photopolarimetric measurement of the Mueller matrix by Fourier analysis of a single detected signal [J]. *Optics Letters* , 2(6), 148. doi: 10.1364/OL.2.000148.

[16] Collins R W, & Koh J. (**1999**). Dual rotating-compensator multichannel ellipsometer: Instrument design for real-time Mueller matrix spectroscopy of surfaces and films [J]. *Journal of the Optical Society of America A* , 16(8), 1997-**2006**. doi: 10.1364/JOSAA.16.001997.

[17] Piller G, Broch L, & Johann L. (**2008**). Experimental study of the systematic errors for a Mueller matrix double rotating compensator ellipsometer [J]. *Physica Status Solidi C* , 5(5), 1027-1030. doi: 10.1002/pssc.200777750.

[18] Li W Q, Zhang C W, Jiang H, Chen X G, & Liu S Y. (**2016**). Depolarization artifacts in dual rotating-compensator Mueller matrix ellipsometry [J]. *Journal of Optics* , 18(5), 055701-055701. doi: 10.1088/2040-8978/18/5/055701.

[19] Qi J, Xue P, Zhang R, An Y Q, Wang Z B, & Li M W. (**2023**). Error correction for Mueller matrix ellipsometry based on a reference optical path [J]. *Applied Optics* , 62(1), 260-265. doi: 10.1364/AO.476005.

[20] Liu S Y, Chen X G, & Zhang C W. (**2015**). Development of a broadband Mueller matrix ellipsometer as a powerful tool for nanostructure metrology [J]. *Thin Solid Films* , 584, 176-185. doi: 10.1016/j.tsf.**2015**.02.006.

[21] Vial A, Grimault A S, Macias D, Barchiesi D, & de la Chapelle M L. (**2005**). Improved analytical fit of gold dispersion: Application to the modeling of extinction spectra with a finite-difference time-domain method [J]. *Physical Review, B. Condensed Matter and Materials Physics* , 71(8), 5416-1-5416-7. doi: 10.1103/PhysRevB.71.085416.

[22] Herzinger C M, McGahan W A, Woollam J A, Paulson W, & Johs B. (**1998**). Ellipsometric determination of optical constants for silicon and thermally grown silicon dioxide via a multi-sample, multi-wavelength, multi-angle investigation [J]. *Journal of Applied Physics* , 83(6), 3323-3336. doi: 10.1063/1.367101.

[23] Huang S H, Zhou Q, & Tan J C. (**2009**). Sensitivity analysis of ellipsometric parameters in ellipsometric spectral measurement [J]. *Journal of Applied Optics* , 30(1), 84-88.

[24] León M, Levcenko S, Serna R, et al. (**2013**). Spectroscopic ellipsometry study of $Cu_2ZnGeSe_4$ and $Cu_2ZnSiSe_4$ poly-crystals [J]. *Materials Chemistry and Physics* , 141(1), 58-62. doi: 10.1016/j.matchemphys.**2013**.04.024.